

The study on steel elliptical cup drawing based on finite element analysis

Jiansheng Xia*, Shasha Dou

Yancheng Institute of Technology, Yancheng City, Jiangsu Province, China

Nanjing University of Aeronautics & Astronautics, Nanjing City, Jiangsu Province, China

Received 1 September 2014, www.cmnt.lv

Abstract

The sheet metal elliptical cup drawing is a complex process, Under the assumption of Prandtl-Reuss flow rule and von Mises yield criterion, the incremental Elasto-plastic large deformation finite element model was established based on the Updated Lagrangian Formulation (ULF). The Elasto-plastic conversions of boundary and deformation are reduced with r_{min} rule. The friction phenomenon of slippage and viscosity at the boundary interface is revised with increment of revision Coulomb rule. The increment rules are led into the whole stiffness matrix, and derived out the stiffness equation. The studies show that the influence on steel elliptical cup drawing deformation is influenced by die structure and parameter. The dates show that finite element simulation and experimental result have a good consistency.

Keywords: elasto-plastic, FEM simulation, elliptical cup drawing

1 Introduction

Sheet metal forming is a common material processing method, which can be divided into stretching, bending, drawing and flanging, etc. The drawing has been widely applied in various applications [1].

Stainless steel is an alloy, which is mainly composed of iron, adding chromium (Cr), nickel (Ni) and other minor elements, and it has some excellent performance, such as: chemical resistance, heat resistance, corrosion. Stainless steel can be roughly divided into 300 and 400 series by chromium and nickel contents. Because of good formability, 300 belongs to Ni series, and drawing parts are used in building materials, kitchen, utensils, pipe fittings, etc. Because of good hardness, 400 belongs to Cr series, and drawing parts are used as decorative purposes or made into tableware, mechanical parts [2].

Zaky [3] 1998 studied the sheet deep drawing of low carbon steel and aluminous plate, found the ideal contour parameters which does not have the lug, and predicted the anisotropy of sheet in forming process.

Hah [4] 2000 studied the failure reasons in the process of drawing forming based on analysis of shell element of finite element, and found the local deformation in long axis, wrinkling in short axis. The reason is the location problem in forming, such as different drawing rates, wrong position between the sheet and die.

Kim [5] 2001 studied the wrinkles problems in the elliptical cup deep drawing based on finite element analysis, proposed the bifurcation-theory for the first time. He mentioned the reasons of causing wrinkles, such as the

stress state, mechanical properties, geometry structure, and contact part of blank and die.

In this paper, the steel sheet 304 cup is analysed with the finite element method, some relationships are studied, such as: relationship between punch load and displacement, distribution of stress and strain, distribution of thickness, and verify by actual experiments. It used to reference for operation process and altered design. Ductile fracture criterion to predict zirconium sheet stretch forming limit. The results show that the extension of zirconium sheet is high, but the stretch is low.

2 Fundamental theory

2.1 VIRTUAL WORK PRINCIPLE

It describes the elastic-plastic deformation with the updated Lagrangian formulation ULF [6], the Virtual work principle formulation can be shown as follows:

$$\int_{V^E} (\ddot{\sigma}_{ij} - e\sigma_{ik}\dot{\epsilon}_{kj})\delta\dot{\epsilon}_{ij}dV + \int_{V^E} \sigma_{jk}L_{jk}\delta L_{ij}dV = \int_{S_f} \dot{f}\delta v_i dS, \quad (1)$$

where, $\ddot{\sigma}_{ij}$ is the Cauchy stress tensor, $\dot{\epsilon}_{kj}$ is the rate of stress tensor, $\dot{\epsilon}_{ij}$ is the strain tensor, σ_{jk} is the rate of strain tensor, $\delta\dot{\epsilon}_{ij}$ is the virtual strain tensor of the point, δL_{ij} is the virtual velocity gradient tensor of the point, δv_i is the velocity component, \dot{f} is surface force component, L_{ij} is velocity gradient tensor, V is unit volume, S is unit surface area.

* *Corresponding author* e-mail: xiajiansheng@163.com

2.2 CONSTITUTIVE RELATION

In preparing the theory of elasto-plasticity, we have made certain assumptions [10]:

- 1) The material is homogeneous and isotropic;
- 2) There is no strain before manufacturing;
- 3) Temperature effect do not consider when manufacturing;
- 4) It obeys the laws of the Hooke's Law in elastic stage;
- 5) It obeys the von Mises yield rule and Prandtl-Reuss plastic flow rule;
- 6) It contains Isotropic strain hardening in constitutive equation;
- 7) There are elastic strain stage and plastic strain stage in material strain rate;
- 8) Punch, die and holder are steel structure;
- 9) The Bauschinger effect do not consider in reverse unloading.

After assuming above, the constitutive relation can be written as follow:

$$\overset{\circ}{\sigma}_{ij} = C_{ijmn}^{ep} \dot{\epsilon}_{mn}, \tag{2}$$

$$C_{ijmn}^{ep} = C_{ijmn}^e - \frac{C_{ijkl}^e C_{uv}^e \frac{\partial f}{\partial \sigma_{kl}} \frac{\partial f}{\partial \sigma_{uv}}}{C_{kluv}^e \frac{\partial f}{\partial \sigma_{kl}} \frac{\partial f}{\partial \sigma_{uv}} + H' \frac{\sigma_{uv}}{\bar{\sigma}} \frac{\partial f}{\partial \sigma_{uv}}}, \tag{3}$$

where $\overset{\circ}{\sigma}_{ij}$ is Jaumann differential of σ_{ij} , C_{ijmn}^{ep} is the elastic-plastic module, C_{ijmn}^e is Elastic module, f is the initial yield function, H' is the strain hardening rate, $\bar{\sigma}$ is Von Mises yield function, so the Matrix form of C_{ijmn}^{ep} can be expressed as bellow:

$$[C^{ep}] = [C^e] - \frac{1}{S} \begin{bmatrix} S_1^2 & S_1 S_2 & S_1 S_3 & S_1 S_4 & S_1 S_5 & S_1 S_6 \\ & S_2^2 & S_2 S_3 & S_2 S_4 & S_2 S_5 & S_2 S_6 \\ & & S_3^2 & S_3 S_4 & S_3 S_5 & S_3 S_6 \\ & & & S_4^2 & S_4 S_5 & S_4 S_6 \\ & & & & S_5^2 & S_5 S_6 \\ & & & & & S_6^2 \end{bmatrix}, \tag{4}$$

symm

where:

$$S = \frac{4}{9} \bar{\sigma}^2 H' + S_1 \sigma'_{xx} + S_2 \sigma'_{yy} + S_3 \sigma'_{zz} + \tag{5}$$

$$2S_4 \sigma'_{yz} + 2S_5 \sigma'_{zx} + 2S_6 \sigma'_{xy},$$

$$S_1 = 2G\sigma'_{xx}, S_2 = 2G\sigma'_{yy}, S_3 = 2G\sigma'_{zz}, \tag{6}$$

$$S_4 = 2G\sigma'_{yz}, S_5 = 2G\sigma'_{zx}, S_6 = 2G\sigma'_{xy}, \tag{7}$$

where σ'_{ij} is deviator of σ_{ij} , G is the friction flow potential, $G = \sigma_1^2 + \sigma_2^2$, $[C^e]$ is the equation in minimum strain, which can be expressed as bellow:

$$[C^e] = \frac{E}{1+\nu} \begin{bmatrix} \frac{1-\nu}{1-2\nu} & \frac{1-\nu}{1-2\nu} & \frac{1-\nu}{1-2\nu} & 0 & 0 & 0 \\ & \frac{1-\nu}{1-2\nu} & \frac{1-\nu}{1-2\nu} & 0 & 0 & 0 \\ & & \frac{1-\nu}{1-2\nu} & 0 & 0 & 0 \\ & & & \frac{1-\nu}{1-2\nu} & 0 & 0 \\ & & & & \frac{1}{2} & 0 \\ & & & & & \frac{1}{2} \\ \text{symm} & & & & & \frac{1}{2} \end{bmatrix}, \tag{8}$$

where E is modulus of elasticity, ν is Poisson's ratio. If the material is homogeneous and isotropic, the Elasto-plastic rate equation can be written:

$$\overset{\circ}{\sigma}_{ij} = \frac{E}{1+\nu} \left[\delta_{ik} \delta_{jl} + \frac{\nu}{1-2\nu} \delta_{ij} \delta_{kl} - \frac{3\alpha \left(\frac{E}{1+\nu} \right) \sigma'_{ij} \sigma'_{kl}}{2\bar{\sigma}^2 \left(\frac{2}{3} H' + \frac{E}{1+\nu} \right)} \right] \dot{\epsilon}_{kl}. \tag{9}$$

If $\alpha = 1$, it is a plastic stage; if $\alpha = 0$, it is an elastic stage or unloading stage.

Equivalent stress and equivalent plastic strain relations can express by n -power law equation:

$$\dot{\sigma} = C (\epsilon_0 + \dot{\epsilon}_p)^n, \tag{10}$$

where C is material constant, n is strain hardening index; $\dot{\sigma}$ is the equivalent stress, $\dot{\epsilon}_p$ is the equivalent plastic strain, ϵ_0 is the initial strain.

2.3 THE FINITE ELEMENT EQUATION

Finite element analysis is the method that the structure is divided into many small units called discrete entity. Based on Large deformation stress and stress rate relation, the finite deformation of Update Lagrangian Formulation, material constitution relationship, the velocity distribution of each unit is show bellow:

$$\{v\} = [N] \{\dot{d}\}, \tag{11}$$

$$\{\dot{\epsilon}\} = [B] \{\dot{d}\}, \tag{12}$$

$$\{L\} = [M] \{\dot{d}\}, \tag{13}$$

where $[N]$ is shape function, $\{\dot{d}\}$ is nodal velocity, $[B]$ is strain rate-velocity matrix, $[M]$ is velocity gradient-velocity matrix.

The principle of virtual work equation and the constitutive equation based on update Lagrangian is linear equation. The formula can be written by the form of incremental representation.

After finite element discrimination, the large deformation rigid general equation is written as bellow:

$$[K]\{\Delta u\} = \{\Delta F\}, \quad (14)$$

where:

$$Q = \begin{bmatrix} 2\sigma_{xx} & 0 & 0 & \sigma_{xy} & 0 & \sigma_{xz} \\ & 2\sigma_{yy} & 0 & \sigma_{xy} & \sigma_{zy} & 0 \\ & & 2\sigma_{zz} & 0 & \sigma_{zy} & \sigma_{xz} \\ & & & \frac{1}{2}(\sigma_{xx} + \sigma_{yy}) & \frac{1}{2}(\sigma_{zx}) & \frac{1}{2}(\sigma_{zy}) \\ & & & & \frac{1}{2}(\sigma_{yy} + \sigma_{zz}) & \frac{1}{2}(\sigma_{xy}) \\ & & & & & \frac{1}{2}(\sigma_{xx} + \sigma_{zz}) \end{bmatrix}, \quad (17)$$

symm

$$Z = \begin{bmatrix} \sigma_{xx} & 0 & 0 & \sigma_{xy} & \sigma_{xz} & 0 & 0 & 0 & 0 \\ & \sigma_{yy} & 0 & 0 & 0 & \sigma_{xy} & \sigma_{yz} & 0 & 0 \\ & & \sigma_{zz} & 0 & 0 & 0 & 0 & \sigma_{xz} & \sigma_{yz} \\ & & & \sigma_{yy} & \sigma_{yz} & 0 & 0 & 0 & 0 \\ & & & & \sigma_{zz} & 0 & 0 & 0 & 0 \\ & & & & & \sigma_{xx} & \sigma_{xz} & 0 & 0 \\ & & & & & & \sigma_{zz} & 0 & 0 \\ & & & & & & & \sigma_{xx} & \sigma_{xy} \\ & & & & & & & & \sigma_{yy} \end{bmatrix}. \quad (18)$$

symm

2.4 FRICTION PROCESSING

There is friction in sheet forming process, so we need to pay attention to materials and tools of the interface conditions [11]. When the material moves along the tool surface curve of the slide, the contact force can be expressed as:

$$F = F_l l + F_n n, \quad (19)$$

where, F_l is radial force and F_n is normal force, and differential equation of F can be expressed as:

$$\dot{F} = \dot{F}_l l + F_l \dot{l} + \dot{F}_n n + F_n \dot{n}, \quad (20)$$

where, differentials of \dot{l} and \dot{n} are expressed as:

$$\dot{l} = -\Delta u_l^{rel} / R, \quad (21)$$

$$\dot{n} = \Delta u_l^{rel} / R, \quad (22)$$

$$[K] = \sum_{(E)} \int_{V^e} [B]^T ([C^{ep}] - [Q])[B] dV + \sum_{(E)} \int_{V^e} [E]^T [Z][E] dV, \quad (15)$$

$$\{\Delta F\} = \sum_{(E)} \int_{S^e} [N]^T \{\dot{f}\} dS \Delta t, \quad (16)$$

$[K]$ is the overall Elasto-plastic stiffness matrix, $\{\Delta F\}$ is the nodal displacement increment, $\{\Delta u\}$ is the nodal forces incremental, $[Q]$ and $[Z]$ are stress correction matrix.

where, R is tool radius, Δu_l^{rel} is the local relative velocity between the tool and node, and the nodes relative speed can be expressed as:

$$\Delta u_l^{rel} = \Delta u_l - \dot{u}_{tool} \sin \theta, \quad (23)$$

where, Δu_l is the contact tangent displacement increment of nodes, \dot{u}_{tool} is the displacement increment of tooling, θ is the rotation angle.

The increment equation of \dot{F} is expressed as follow:

$$\dot{F} = (\dot{F}_l - F_n \Delta u_l / R + F_n \dot{u}_{tool} \sin \theta / R) \cdot l + (\dot{F}_n - F_l \Delta u_l / R - F_l \dot{u}_{tool} \sin \theta / R) \cdot n. \quad (24)$$

Rigid matrix governing equation of the contact nodes is expressed bellow:

$$\begin{bmatrix} K & \dots \\ \dots & K_{11} + F_n / R & K_{12} \\ \dots & K_{21} + F_n / R & K_{22} \end{bmatrix} \begin{Bmatrix} \dots \\ \Delta u_l \\ \dots \\ \Delta u_n \end{Bmatrix} = \begin{Bmatrix} \dots \\ \dot{F}_l + F_n \dot{u}_{tool} \sin \theta / r \\ \dots \\ \dot{F}_l - F_n \dot{u}_{tool} \sin \theta / r \end{Bmatrix} \quad (25)$$

2.5 INCREMENTAL STEPS OF r_{min} METHOD

Using the elastic plastic finite element method with large deformation method, also called the Yamada r_{min} method. Each incremental step value is equal to incremental displacement of initial deformation increment of the tooling. Adopting the method of updated Lagrangian formulation, calculating each increment of displacement, strain, stress, load, springback value after forming the final shape of sheet metal in unloading condition, the value of load incremental in each step is controlled by r_{min} equation, which is shown as bellow:

$$r_{min} = MIN(r_1, r_2, r_3, r_4, r_5), \quad (26)$$

where, r_1 is The maximum allowable strain increment, r_2 is the maximum allowable rotation increment, r_3 is the minimum value in all elastic elements, r_4 is contact position between free node and tooling, r_5 is discont position between free node and tooling.

3 Numerical analysis flow

Based on the finite deformation theory, ULF equation and r_{min} method, a set of effective analysis of sheet metal forming process is established. Firstly, a 3d part and mold is designed with the NX software, and then mesh them with NASTRAN software. Secondly, the meshed models are drawn into the data file and did finite element analysis. The simulation flow chart is shown in Figure 1.

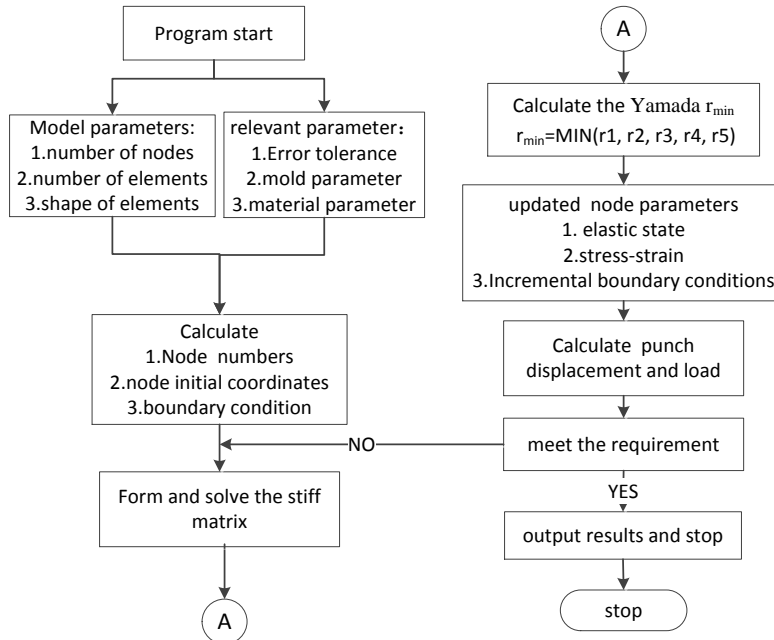


FIGURE 1 Numerical simulation of flow chart

Based on the theory upwards, the research of steel elliptical cup drawing is studied, including relationship between the punch load and displacements, stress and strain, thickness, spring-back and warpage. Simulation experimental parameters were carried out, which are friction coefficient (μ), punch radius (r_p), die radius (R_d). The parameters of warpage problems are verified by the experiment are optimized and served a reference for drawing designer.

The whole structure is composed of punch, die and blank holder. The model picture was shown as Figure 2.

The initial relation of part and die is shown in Figure 2a, also, the punch down a certain travel case is shown Figure 2b. It takes two coordinates to solve the problem, which are fixed coordinates (X, Y, Z) and local coordinates (ξ, η, ζ). It uses the fixed coordinates (X, Y, Z) when nodes do not contact with the tool, and uses the local coordinates (ξ, η, ζ) when nodes contact with the tooling. Using coordinates rule based on the right-hand rule. L-axis is the

tangential direction of contact line between the part and tools when n-axis is the normal direction.

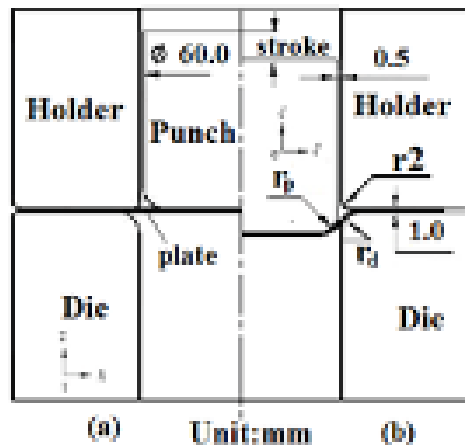


FIGURE 2 Sheet metal and die size chart: a) before deformation, b) after deformation

The contact condition of each node of plates will change depending on deformation in sheet metal forming. When the displacement increment is zero, the boundary conditions of increment displacement of the next node will changes to free node boundary conditions. When sheet contacts the tools, contact condition is changed to the boundary conditions, which bases on the generalized r_{min} method.

The SUS304 material stainless steels are provided by a steel Crop, of which the chemical and mechanical properties as shown in Table1 as bellow [9].

TABLE 1 Mechanical properties of SUS304

stress-strain relationship: $\bar{\sigma}=1400(0.024+\bar{\epsilon}_p)$	
initial thickness: $t = 0.8\text{mm}$	Poisson's ratio: $\nu = 0.3$
yield stress: $\sigma_y = 315\text{MPa}$	coefficient of friction: $\mu = 0.1$
Yang coefficient: $E = 2.1 \times 10^5 \text{MPa}$	fractured thickness: $t_f = 0.536\text{mm}$

Because of the symmetrical sheet model, 1/4 model is taken to analysis.

It uses the quadrilateral segmentation of degenerated shell element in sheet metal meshing, when the die meshing uses the triangle segmentation (Table 2).

TABLE 2 The finite element mesh dates of punch, die and sheet

Name	Element type	Element number	Node number
Punch	Triangle	1356	569
Die	Triangle	1638	749
Holder	Triangle	813	426
Blank	Four-node shell element	1478	1321

4 Results

4.1 DISTRIBUTION OF STRESS AND STRAIN

The analysis in elliptical cup drawing process generally can be divided into three stages.

The first stage: Punch and sheet mental just begins to contact, when the stroke is 5mm. The stress distribution of elliptical cup drawing is as shown in Figure 3a. As can be seen from the figure, the normal stress occurs around the punch fillet, the concentration tensile stress appears in long axis centre.

The second stage: when the stroke is 30.0mm, the stress distribution of elliptical cup drawing is as shown in Figure 3b. As can be seen from the figure, the side wall of the sheet gradually forms to straight wall of elliptical cup along the punch. As the sheet flow into the die and deform plastically the punch load increases. The normal stress also occurs in the sheet between the holder and punch, and tensile stress occurs in the straight wall of elliptical cup which had flowed into the die.

The third stage: this is the finish stage in drawing. The stress distribution of elliptical cup drawing is as shown in Figure 3c, the stress concentration occurred in punch fillet, and the maximum value is in the top of the cup, which is 1560MPa.

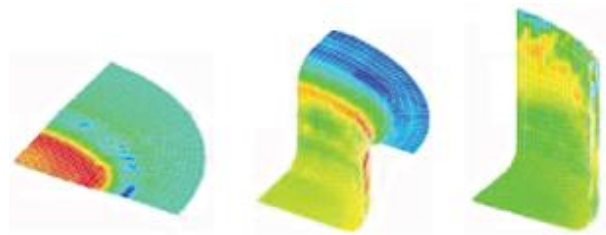


FIGURE 3 Stress distribution: a) stroke = 0.05mm, b) stroke = 30mm, c) finish stroke

4.2 PUNCH LOAD ANALUSIS ANALYSIS

When the elliptical cup forming, the sheet will be under a lot of stress, such us the tensile load of the punch moving down, the friction between the die and sheet, the compression force caused by sheet diameter reduced gradually. The punch force increases with the punch stroke firstly. The maximum value is 78kN, when the stroke is 28mm. Next, the value decreases with the increase of stroke. Numerical analysis and experimental results are as shown in Figure 4.

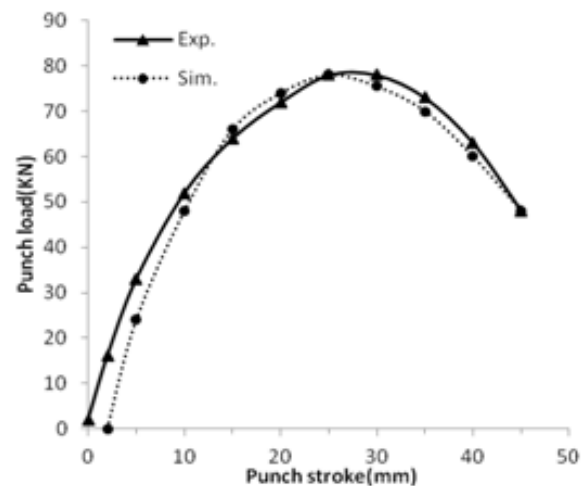


FIGURE 4 The relationship of punch load and stroke

4.3 THICKNESS CHANGE ANALYSIS

The sheet mental is used to do drawing experiment analysis, of which the diameter is 105mm. The thickness data are measure along the direction of long-axis and short-axis and as shown in Figure 5. As can be seen from the figure, the thinnest thickness is in the bottom area near the long-axis fillet, which is the 0.58mm and slightly larger than the rapture thickness, then the drawing part can be finished.

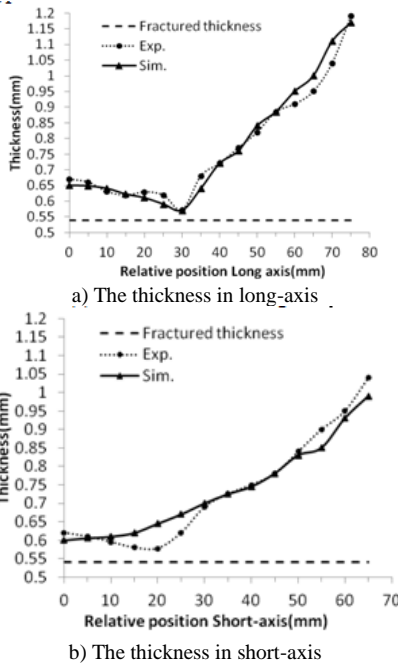


FIGURE 5 Thickness change analysis in long axis and short axis

4.4 FORMING LIMIT ANALYSIS

In order to find out the limit thickness of elliptical flange, some experiments are carried out with the different diameters of sheet, and set the value 0.41mm as the criterion of rupture. If the thickness is thinner, the program will judge that the sheet is in the limit thickness. FR (Forming ratio) LFR (Limit Forming Ratio), and EFR (Excessive Forming Ratio) are referred by Huang and Chen [9].

DR (Drawing Ratio), LDR (Limit Drawing Ratio) and EDR (Excessive Drawing Ratio) are used to calculate and judge, which are defined by Huang [9]:

$$FR = \frac{D_p}{D_h} = \frac{C_p}{C_h}, \tag{27}$$

$$LFR = \frac{D_p}{D_{h,min}} = \frac{C_p}{C_{h,min}}, \tag{28}$$

$$EDR = \frac{D_p}{D_{h,f}} = \frac{C_p}{C_{h,f}}, \tag{29}$$

where, D_p is the diameter of punch; D_h is the diameter of sheet with necking or fracture; $D_{h,min}$ is the maximum diameter of sheet without necking or fracture; D_p is the perimeter of the elliptical punch; $D_{h,f}$ is the perimeter of the sheet without necking or fracture; C_p is the circumference of punch, C_h is the circumference of initial inner elliptical hole with necking or fracture; $C_{h,min}$ is the maximum the circumference of initial inner elliptical hole without necking or fracture; $C_{h,f}$ is circumference of initial inner elliptical hole with part necking or fracture.

The experimental arrangement of sheet blank diameter: $\phi 105\text{mm} \rightarrow \phi 106\text{mm} \rightarrow \phi 107\text{mm}$, and definition $DR = 2.116$ (blank diameter = 105mm), $LDR = 2.135$ (blank diameter = 106mm) and $EDR = 2.168$ (blank diameter = 107mm).

The thickness distribution of long and short axis which the blank diameter is 107mm is shown in Figure3. As can be seen from the figure, because of pinching-out, there is necking and rupture at the relative position 29mm in the long-axis.

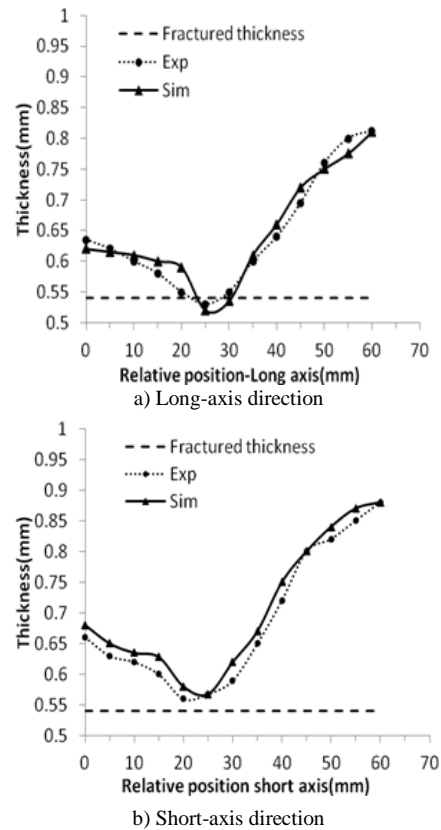


FIGURE 6 The distribution of thickness

The other simulation experiments are carried out. It is found that the minimum thickness is 0.55mm along the long-axis or short-axis with the blank diameter 106mm. The thickness is very close to the rupture, and reaches the limit.

4.5 LIMIT DRAWING COEFFICIENT ANALYSIS

In order to study the relationship between the limit drawing ratio and punch or die fillet radius, eight groups' experiments are carried out. The punch radius and die fillet are 3.0mm, 5.0mm, 7.0mm and 9.0mm, respectively. The results are as shown in Table3 as bellow.

As can be seen from the Figure 7, when punch radius increases from 3.0mm to 9.0mm, the limit drawing ratio also increases from $LDR = 2.1$ to $LDR = 2.157$. When die radius increases from 3.0mm to 9.0mm, the limit drawing ratio LDR also increases from 2.07 mm to 2.181mm.

TABLE 3 Limit drawing ratio with the different radius of punch and die

Radius(mm)	3.0	5.0	7.0	9.0
Rp=5.0mm	2.12	2.135	2.148	2.156
Rd=5.0mm	2.06	2.135	2.163	2.18

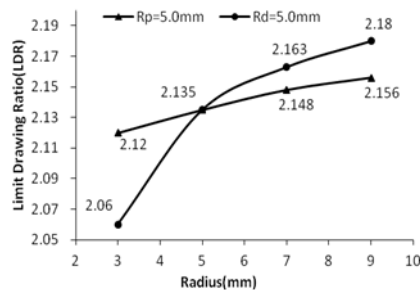


FIGURE 7 The relationship between the limit drawing ratio and radius of punch or die

5 Conclusion

Based on the numerical analysis and experimental results, combined with finite element method with the incremental Elasto-plastic theory, analysed warpage phenomenon in stainless steel elliptical cup drawing process, the following conclusions are obtained.

1) The punch load increase with the increase of punch stroke. When the stroke is 27.0mm, the maximum punch load is 78.0kN, which is close to actual experimental data.

References

- [1] Xia J S, Dou S S 2013 Experimental Research on the Flanging Height Adjustment Based on Environmental Way *International Journal of Applied Environmental Sciences* **8**(20) 2470-89
- [2] Huang Y M, Chen T C 2005 Influence of Blank Profile on the V-Die Bending Camber Process of Sheet Metal *International Journal of Advanced Manufacturing Technology* **25**(7) 668-77
- [3] Zaky A M 1998 Optimum Blank Shape of Cylindrical Cups in Deep Drawing of Anisotropic Sheet Metals *Journal of Materials Processing Technology* **76**(1) 203-211
- [4] Huh H, Kim S H, Kim S H 2000 Process Design For Multi-Stage Elliptic Cup Drawing with the Large Aspect Ratio *European Congress on Computational Methods in Applied Sciences and Engineering* **8**(11) 1-16
- [5] Kim H B, Yoon J W, Yang D Y, Barlat F 2001 Investigation into Wrinkling Behavior in the Elliptical Cup Deep Drawing Process by Finite Element Analysis using Bifurcation-Theory *Journal of Materials Processing Technology* **111**(1) 170-4
- [6] Huang Y M, Chien K H 2001 Influence of the Punch Profile on the Limitation of Formability in Hole-Flanging Process *Journal of Materials Processing Technology* **113**(1) 720-4
- [7] Takuda H, Hatta N 1998 Numerical Analysis of Formability of a Commercially Pure Zirconium Sheet in Some Forming Processes *Materials Science and Engineering* **242**(1) 15-21
- [8] Leu D K 1996 Finite-Element Simulation of Hole-Flanging Process of Circular Sheets of Anisotropic Materials *International Journal of Mechanical Sciences* **38**(8) 917-33
- [9] Huang Y M, Chien K H 2002 Influence of Cone Semi-Angle on the Formability Limitation of the Hole-Flanging Process *International Journal of Advanced Manufacturing Technology* **19**(8) 597-606
- [10] Sousa L C, Castro C F, Antonio C A C 2006 Optimal Design of V and U Bending Processes Using Genetic Algorithms *Journal of Material Processing Technology* **172**(1) 35-41
- [11] Liu G, Lin Z, Xu W, Bao Y 2002 Variable Blankholder Force in U-Shaped Part Forming for Elimination Springback Error *Journal of Material Processing Technology* **120** 259-64
- [12] Samuel M 2000 Experimental and numerical prediction of springback and side wall curl in u-bending of anisotropic sheet metals *Journal of Materials Processing Technology* **105** 382-93

Authors



Jiansheng Xia, born in September, 1980, Yancheng, Jiangsu Province, P.R. China

Current position, grades: lecturer at Yancheng Institute of Technology, China.

University studies: MSc at Northeast Agricultural University in China.

Scientific interests: mold design, CAD/CAE/CAM technologies.

Publications: more than 10 papers.

Experience: teaching experience of 8 years, 2 scientific research projects.



Shasha Dou, born in December, 1982, Yancheng, Jiangsu Province, P.R. China

Current position, grades: lecturer at Yancheng Institute of Technology, China.

University studies: MSc at Shandong University of Technology in China.

Scientific interests: plastic mold design, CAD/CAE/CAM technologies.

Publications: more than 10 papers.

Experience: teaching experience of 8 years, 1 scientific research project.